Water Resources Variability in Africa during the XXth Century (Proceedings of the Abidjan'98 Conference held at Abidjan, Côte d'Ivoire, November 1998). IAHS Publ. no. 252, 1998.

Interannual variability in rainfall, water vapour flux, and vertical motion over West Africa

MARYBETH LONG, DARA ENTEKHABI

48-331 Ralph M. Parsons Laboratory, Massachusetts Institute of Technology, Cambridge, Massachusetts 02139, USA

e-mail: darae@mit.edu

SHARON E. NICHOLSON

Department of Meteorology, Florida State University, Tallahassee, Florida 32306, USA

Abstract This study examines how local and large-scale forcing mechanisms contribute to the initiation and maintenance of drought conditions in sub-Saharan Africa. The analysis uses 31-year datasets of rainfall, moisture flux, and vertical motion. Empirical orthogonal functions (EOFs) of the 500 mb vertical wind velocity indicate major modes of variability in large-scale general circulation features (e.g. Hadley/Walker circulation). The data record includes both pluvial and drought periods, and enables distinctions between the early and late rainy season, and between northern and southern sub-Saharan regions. Results suggest that, while changes in Sahelian rainfall often accompany shifts in the general circulation, land surface forcing mechanisms may stabilize dry regimes and override the effects of large-scale changes. Time series of rainfall and vertical motion patterns show that anomalous general circulation features produced a state conducive to dry conditions prior to multi-year drought in the late 1960s. Land surface forcing may have helped to perpetuate this dry regime through the 1970s, despite the presence of large-scale features normally associated with wetter conditions.

INTRODUCTION

The West African drought of the past three decades has had devastating social and environmental impacts and has prompted considerable research. Yet, the causes of West African drought remain elusive (Nicholson, 1989; Rowell *et al.*, 1995). This study aims to advance understanding of these causes by asking:

(a) How do large-scale and local-scale forcing mechanisms affect rainfall?

(b) At what times during the rainy season do large-scale and local-scale mechanisms operate? and

(c) In what locations within West Africa are these mechanisms most prominent?

We address these questions by comparing the behaviour of rainfall, horizontal moisture transport, and vertical motion. The analysis also includes temporal comparisons between June/July (JJ) and August/September (AS) periods of the rainy season, and spatial comparisons between northern and southern regions of sub-Saharan Africa. The data set consists of 31-year time series of rainfall, vertically integrated moisture flux, and dominant modes of vertical wind velocity fields. These times series cover both drought and pluvial periods. Results suggest that, while changes in Sahelian rainfall often accompany shifts in the general circulation, landatmosphere interactions may intensify drought and contribute to its persistence, especially during the late rainy season.

DATA

The period of analysis is dictated by the rainfall data set which extends from 1959 through 1989 for south and north sub-Sahara regions. The north sub-Sahara (north) lies between approximately 25° and 15°N latitude. The south sub-Sahara (south) lies between approximately 15° and 7.5°N latitude. These areas generally experience a high-sun rainy season between June and September with the maximum rainfall occurring in August. Because the rainfall data set does not include the Sahelian wet period during the early 1950s, the study is not a totally comprehensive analysis of wet versus dry years. Time series of June/July (JJ) and August/September (AS) rainfall for north (Fig. 1) and south (not shown) were used to subjectively delineate extended "wet" and "dry" periods for comparison and contrast.

Horizontal water vapour flux vectors **Q** were obtained by vertically integrating meridional and zonal flux over pressure levels. These meridional and zonal **Q** components were also averaged over time. Dr Abraham Oort of the National Oceanic and Atmospheric Administration (NOAA) Geophysical Fluid Dynamics Laboratory (GFDL) provided the specific humidity, wind, and vertical velocity data. The data are monthly mean values for the years 1959 to 1989, inclusive. The data are based on radiosonde measurements taken at eight pressure levels: 1000, 950, 900, 850, 700, 500, 400, and 300 millibars (mb) and interpolated onto a 2.5 latitude by

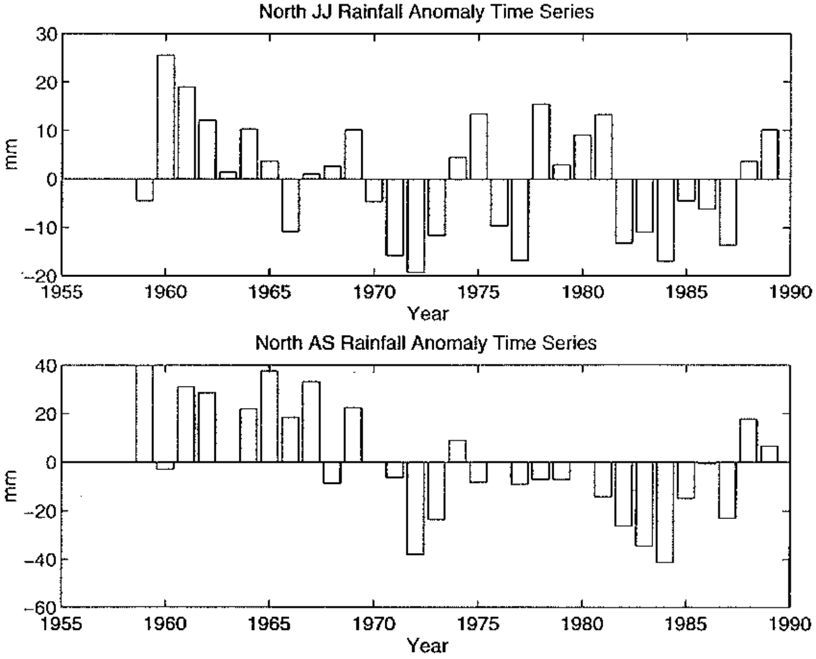
North JJ Rainfall Anomaly Time Series

North AS Rainfall Anomaly Time Series

Fig. 1 North rainfall anomaly time series shows regionally-averaged departures from regionally-averaged long-term (31-year) means.

5 longitude grid using CRAM (Conditional Relaxation Analysis Method), an objective analysis scheme detailed in Oort (1983).

WATER VAPOUR FLUX ANALYSIS

Figure 2 shows a time series of JJ and AS meridional flux at 7.5°N latitude. The plotted values represent the total meridional flux of water vapour passing a unit length of the 7.5°N latitude boundary per unit time. The lines overlaying the bar graphs represent the wet-period and dry-period means for each season. Dry years exhibit lower mean meridional flux in both JJ and AS. Differences between wet and dry-year mean meridional flux values are statistically significant at a 95% confidence level based on a two-way t-test of the differences in the means. Differences in wet and dry-year mean meridional flux may reflect weakening of the Hadley cell circulation during drought years (Kidson, 1977; Fontaine & Janicot, 1992). It should be noted, however, that no correspondence appears between the general circulation and rainfall in individual years. A figure of JJ and AS meridional flux at 15°N latitude (not shown) also indicates northward movement of the ITCZ during summer months. During JJ, the convergence zone is to the south of 15°N and a northerly flux dominates meridional motion.

EOF ANALYSIS OF VERTICAL MOTION

Empirical orthogonal function (EOF) (eigenvector) analysis was used to derive a scalar index of the general circulation field from the gridded vertical velocity (Ω)

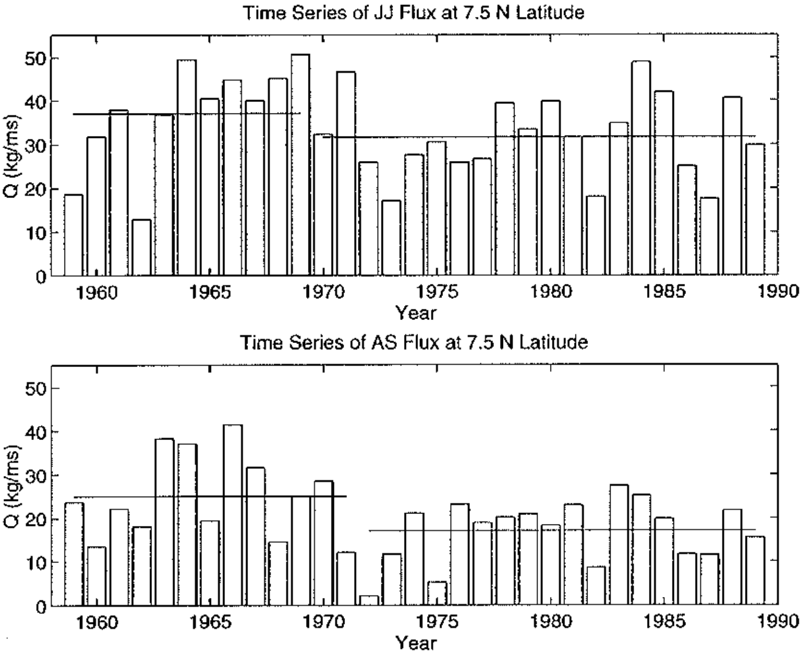

Fig. 2 Time series of meridional moisture flux at 7.5°N. Solid lines represent mean values for wet and dry years. Wet and dry-year means (in both JJ and AS) differ significantly at the 95% level based on a two-way t-test.

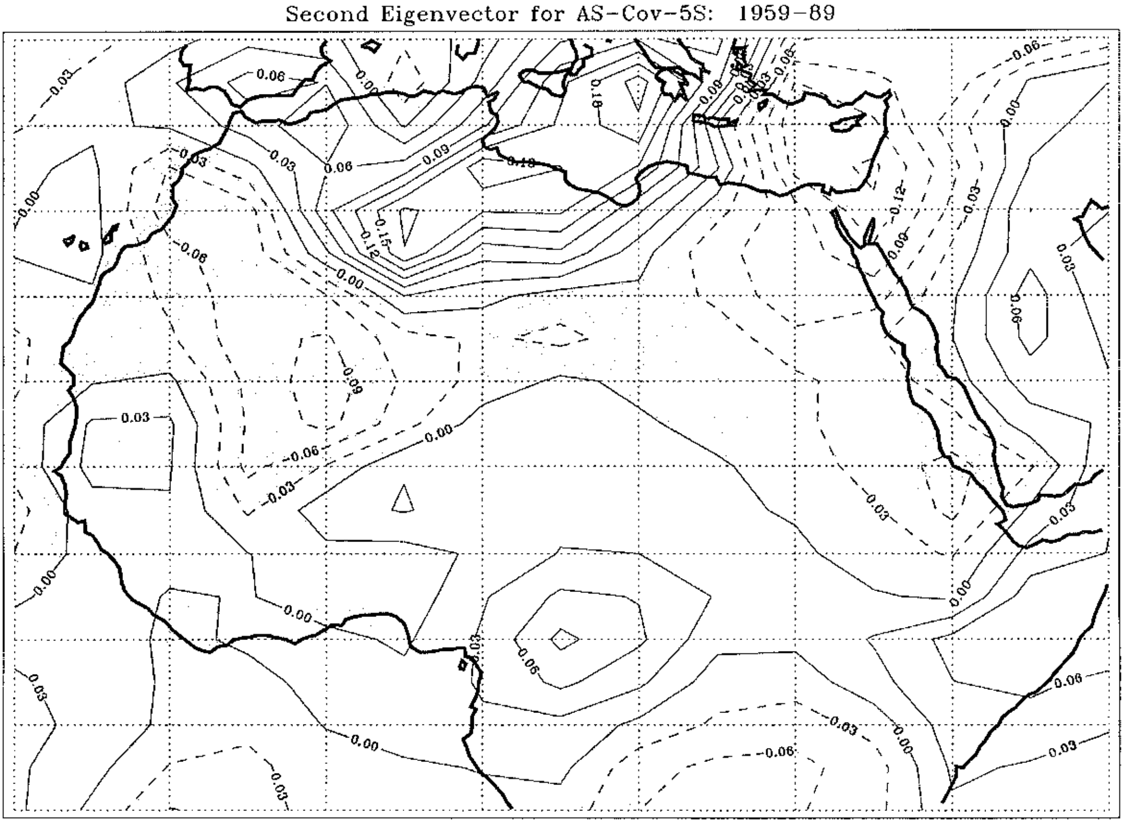

Fig. 3 Second eigenvector pattern (AS-EOF2) calculated from the covariance matrix of the AS vertical velocity field at 500 mb. This pattern exhibits adjacent positive and negative regions that extend from east to west across the north of the continent.

field. Eigenvectors were calculated using the covariance matrix of 500 mb omega values between 20°E and 50°W longitude and between 5°S and 40°N latitude. Thirty-one year means were removed from each element of the matrix to form matrix **F**. EOF calculations were performed on the covariance matrix formed from matrix **F** and its transpose. Both rotated and unrotated EOFs were examined.

AS-EOF1 (not shown) represents about 17% of the total variance in AS and exhibits a double dipole structure. A strong north–south dipole suggestive of Hadley-type overturning is present in the east, but an east–west dipole suggestive of Walker-type overturning is evident across the Sahel. Thus, EOF1 may reflect a combined Hadley/Walker cell pattern, which has consistent seasonal dynamics and spatial orientation. AS-EOF2 (Fig. 3) reflects roughly 15% of the total variance and shows a strong north–south dipole over West Africa, although it is not zonally symmetric.

JJ and AS multiplier time series for EOF1 patterns (Fig. 4) exhibit a low frequency pattern and collapse in the mid-1960s, a few years before the onset of drought in the late 1960s. The EOF2 time series in both JJ and AS (Fig. 5) show a similar collapse in the mid-1960s, but another reversal in the mid-1970s.

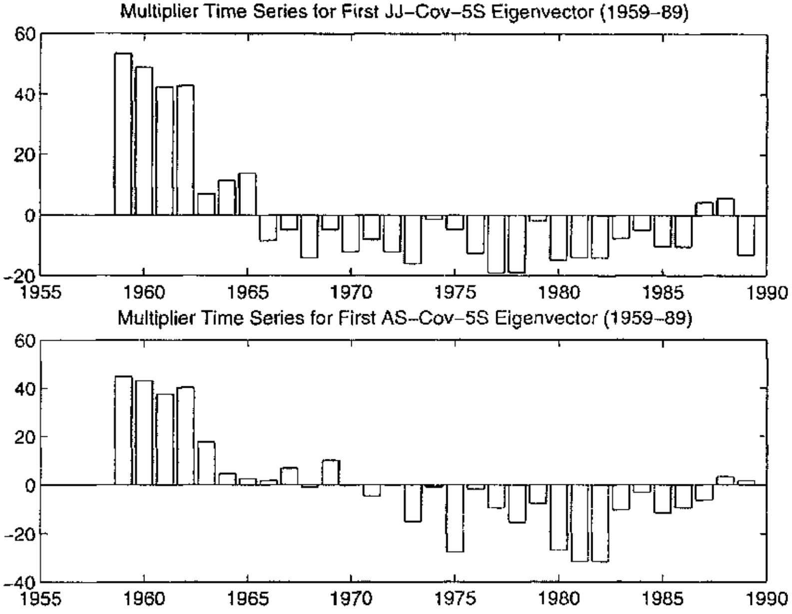

Fig. 4 Time series showing multipliers of the AS-EOF1 eigenvector. This time series collapses in the mid-1960s, a few years before the onset of drought in the late 1960s.

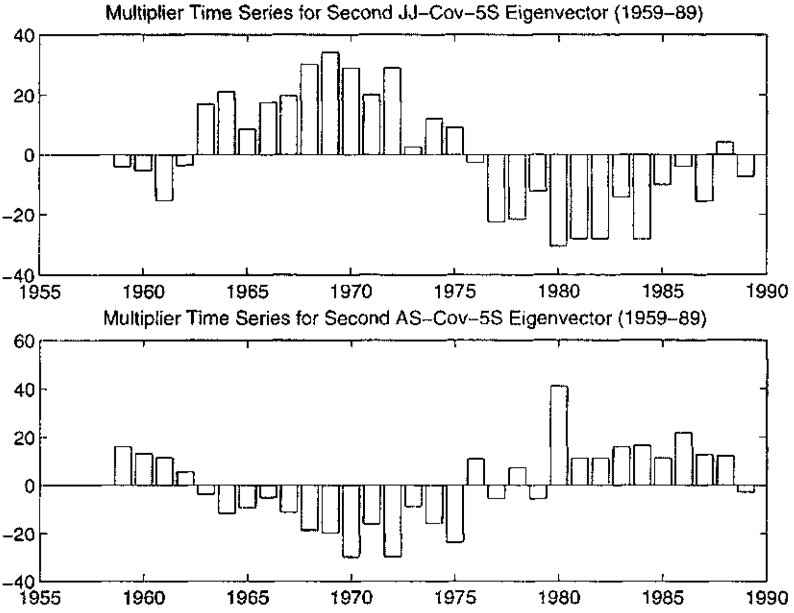

Fig. 5 Time series showing multipliers of the AS-EOF2 eigenvector. This time series exhibits a low frequency pattern, with marked shifts in the mid-1960s and mid-1970s.

COVARIABILITY OF VAPOUR FLUX, RAINFALL, AND VERTICAL MOTION

Linear correlation coefficients were determined for rainfall and vapour flux times series, for rainfall and vertical motion (i.e. for rainfall and EOF multiplier time series), and for vertical motion and vapour flux time series. Each pair of variables was correlated at the following intervals: –2, –1, 0, 1, 2. A negative sign indicates that one parameter lags the other, a positive value indicates that the same parameter leads the other, and zero indicates one-to-one correlation.

Correlation coefficients for rainfall and vertical motion EOF time series show that rainfall has a stronger relationship with EOF1 than with EOF2. EOF1 *leads* rainfall by one to two years in both regions and seasons at the 98% significance level. EOF1's southeast/northwest dipole pattern may represent Hadley/Walker partitioning, and the EOF1 time series shows a collapse in the strength of this dipole in the mid-1960s. This suggests that a weakening of the Hadley/Walker system *preceded* drought.

Correlation results suggest that meridional flux forces rain in the north, with the strongest forcing in AS. Zonal flux forces rainfall in the South during AS. A possible interpretation is that the ITCZ, with its north/South anomalous position, is responsible for the majority of rainfall variability in the north, while the AEJ and its attendant pressure disturbances (wave guide) have greater influence on the South region's rainfall.

Scale of fluctuation values (Table 1) indicate that rainfall and water vapour flux are less persistent in JJ than in AS. This lower persistence in JJ rainfall is noted above and may reflect random onset of the rainy season. One interpretation suggests that higher persistence in AS may indicate local-scale (land) forcing mechanisms resulting from anomalies triggered by large-scale general circulation or air-sea interaction forcing. Other factors could include feedbacks involving radiation and cloud microphysics that are affected by surface dryness, albedo, and dust generation. However, persistent SST patterns cannot be ruled out as a causal factor.

Table 1 Scale of fluctuation values show that rain and water vapour flux are less persistent in JJ than in AS. Lower persistence in JJ rainfall may reflect random onset of the rainy season. Higher AS persistence may reflect local land-forcing mechanisms.

Parameter	JJ North	JJ South	AS North	AS South
Rainfall	1.3	1.3	2.8	4.1
Zonal flux	1.3	1.6	1.7	2.0
Meridional flux	1.0	1.2	1.6	1.7

Differences in rain and vapour flux persistence suggest that general circulation features play an important drought-forcing role. During JJ, rainfall and vapour flux have similar time scales. However, during AS, rainfall persistence exceeds persistence in meridional and zonal vapour flux. This, along with the above-mentioned rainfall/flux correlations, suggests that general circulation features such as the ITCZ and AEJ force rainfall during JJ. However, during AS additional mechanisms operate in conjunction with the ITCZ and the AEJ to influence rainfall and give it persistence greater than that evident in forcing mechanism themselves.

SUMMARY AND CONCLUSIONS

In the north and South sub-Sahara and in both JJ and AS, the EOF1 time series (Fig. 4) leads that of rainfall by one to several seasons. This suggests a marked change in the rainfall regime prior to drought onset and suggests that anomalous general circulation features produced a state conducive to dry conditions. Correlation values also attest to a correspondence between rainfall and meridional vapour flux at 15° and suggest dependence between the ITCZ and rainfall in the north. In the South, significant correlations between AS rainfall and zonal flux indicate dependence between the strength of easterly flow and AS rainfall. However, there is no evident correspondence between the general circulation parameters studied and rainfall anomalies in individual years.

The EOF2 time series (Fig. 5), indicative of a Hadley/Walker circulation, collapses in the mid-1960s and again in the mid-1970s. This implies that a major circulation shift that took place in the mid-1970s was not accompanied by a shift to a "wet" rainfall regime. It is interesting to note that around the mid-1970s a shift occurred to wetter conditions over southern Africa and to higher SSTs in the equatorial Atlantic and Indian Oceans. Prior to this time, the rainfall trends in the Sahel and southern Africa paralleled each other and mirrored the SST patterns. When SSTs cooled in the mid-1970s and rainfall increased in southern Africa, rainfall likewise increased in the Sahel. However, increased rainfall in the Sahel was only temporary and dry conditions returned. This suggests that land surface forcing stabilized the dry regime in the mid-1970s such that a shift in the large-scale circulation, normally linked to wetter conditions, was insufficient to push the Sahel to a "wet" mode.

Scale of fluctuation values for vapour flux and rainfall also provide evidence of land surface feedback mechanisms. While moisture flux and rainfall exhibit similar levels of persistence in JJ, rainfall persistence exceeds vapour flux persistence in AS.

REFERENCES

Fontaine, B. & Janicot S. (1992) Wind-field coherence and its variations over West Africa. *J. Climate* 5, 521–523.

Kidson, J. W. (1977) African rainfall and its relation to upper air circulation. *Quart. J. Roy. Met. Soc.* **103**, 441–456.

Nicholson, S. E. (1989) African drought: characteristics, causal theories, and global teleconnections. *AGU Geophysical Monographs* **52**, 79–100.

Oort, A. H. (1983) Global Atmospheric Circulation Statistics, 1958–73. *NOAA Prof. Pap. 14, Geophysical Fluid Dynamics Laboratory, New Jersey, USA.*

Rowell, D. P, Folland, C. K., Maskell, K. & Ward, N. (1995) Variability of summer rainfall over tropical North Africa (1906–92): observations and modelling. *Quart. J. Roy. Met. Soc.* **121**, 669–704.